Tetrahedron 75 (2019) 2965–2970

Contents lists available at ScienceDirect

Tetrahedron

journal homepage: www.elsevier.com/locate/tet

Computational and cyclic voltammetry studies of high effective-molarity assisted reversible reductions of [4]- and [5] heli-viologens: Potential building blocks for new materials

Xiaoping Zhang, Edward L. Clennan*, Toby Petek

Department of Chemistry, University of Wyoming, Laramie, WY, 82071, USA

ARTICLE INFO

Article history:
Received 25 February 2019
Received in revised form
6 April 2019
Accepted 16 April 2019
Available online 20 April 2019

Keywords:
Viologen
Helicene
Cyclic voltammetry
Reduction

ABSTRACT

Computational and cyclic voltammetry studies have been used to explore electrochemical reductions of three helically chiral homologues, $\mathbf{2}^{2+}$, $\mathbf{3}^{2+}$, and $\mathbf{4}^{2+}$, of methyl viologen. Thermochemical-electrochemical cycles are used as frameworks to describe the reversible redox properties of these helically chiral viologens as novel reversible four-sided ECEC (**E**lectron-transfer **C**hemical-reaction **E**lectron-transfer **C**hemical-reaction) processes.

1. Introduction

Methyl viologen or paraquat, $\mathbf{1}^{2+}$ (Chart 1), has been known since 1882 [1]. The importance of these 4,4′-bipyridinium salts as electron transfer mediators [2,3], as herbicides [4], as components of electrochromic displays [5] and supramolecular structures [6–9], and as probes to study zeolites [10] and DNA [11], is amply documented in several manuscripts and excellent reviews. Most of these applications take advantage of the ability of viologens to exist in dicationic, radical cation, and neutral redox states (Chart 1). For example, $\mathbf{1}^{2+}$ has been incorporated into Blue Box [12–14], ExBox [15], and ExCage [9] for molecular recognition applications, $\mathbf{1}^{+\cdot}$ has been used as an integral part of molecular machines [16], and the 2,2′-analogues of 4,4′-dimethyl-4,4′-bis-pyridinylidene, $\mathbf{1}^{0}$, are used as potent organic reducing agents [17].

The two redox couples (dication → radical-cation and radical-cation → neutral) for methyl viologen, $\mathbf{1}^{2+}$, and for most viologens are both chemically and electrochemically reversible in organic solvents [18], and the differences in their standard redox potentials ($E_1^o - E_2^o$) are too large for significant disproportionation of two viologen radical-cations to form the dication and neutral redox states. For example, the disproportionation equilibrium constant for methyl viologen radical cation, $\mathbf{1}^{+\cdot}$, is only 1.7×10^{-7} in acetonitrile [19]. However, in polar solvents that dampen repulsive Coulombic forces, the radical cations, assisted by dispersion forces, form weak π-bonded dimers historically referred to as pimers [20].

The recent introduction of N,N′-dialkylated 4,4′-bipyridinium ions $\mathbf{2}^{2+}$, $\mathbf{3}^{2+}$, and $\mathbf{4}^{2+}$ [21], (Chart 2) provides the opportunity to build chiral analogues of achiral viologen materials. A key step in this construction process is an examination of the electrochemical behaviours of $\mathbf{2}^{2+}$, $\mathbf{3}^{2+}$, and $\mathbf{4}^{2+}$ to determine if the redox switchable, chemically stable, dication, radical cation, and neutral redox partners observed in methyl viologen, (vide supra) are accessible in these novel helically chiral analogues [18].

2. Results and discussion

The structures of the dication, radical cation, and neutral redox states were located and minimized for viologens **2**, **3**, and **4** using the B3LYP/6-311 + G(2d,p) computational model. The helical framework prevents the viologen core from adopting the energetically preferred structure of methyl viologen ($\mathbf{1}^{2+}$). For example, the inter-pyridinium-ring-pyridinium-ring dihedral angle (angle a-b-c-d in Chart 1) of 41.9° in methyl viologen is significantly constrained to 25.2°, 15.8°, and 15.2° in $\mathbf{2}^{2+}$, $\mathbf{3}^{2+}$, and $\mathbf{4}^{2+}$, respectively.

* Corresponding author.
E-mail address: clennane@uwyo.edu (E.L. Clennan).

https://doi.org/10.1016/j.tet.2019.04.043
0040-4020/

The pyridinium rings in the helicene dications, radical cations, and neutral redox structures are also significantly distorted from planarity. In $\mathbf{2}^{2+}$, $\mathbf{3}^{2+}$, and $\mathbf{4}^{2+}$, the average of the 12 inter-ring dihedral angles (e.g. angle a-b-e-f in Chart 1) in the two pyridinium-rings are 9.4°, 6.9°, and 5.4°, respectively. In contrast, in $\mathbf{1}^{2+}$ the two pyridinium rings are nearly planar with an average intra-ring dihedral-angle of 0.3°. Framework induced bending of the pyridinium rings is also observed in the radical cations and neutral redox partners. The average intra-pyridinium-ring dihedral angles are 0.3°, 10.8°, 7.5°, 6.1°, and 2.6°, 13.0°, 8.7°, 7.0° in the radical cation and neutral redox states of **1**, **2**, **3**, and **4**, respectively. The global minimum for $\mathbf{1}^{0}$ adopts a C_2 symmetric structure with the two N-methyl groups bent out of the plane of the heterocyclic rings on opposite faces of the viologen.

In order to estimate the energetic cost of these deformations the viologen cores were excised from the minimized structures of the heli-viologens, the severed C–C bonds were replaced with 1.070 Å long C–H bonds, and single point energies were calculated at the B3LYP/6-311 + G(2d,p) level. The calculated relative viologen-core distortion energies are given in Table 1. The energetic cost of embedding the three redox partners into helical scaffold **2**, **3**, or **4** decreases in the order dication > radical cation > neutral, which also coincides with decreasing aromatic-character of the three redox states (See Chart 1). In addition, the energetic cost of distortion decreases in the order **2** > **3** > **4** > **1**(reference) in all three redox states. This sequence also represents the decrease in distortion of the nitrogen containing rings from planarity (vide supra).

In order to investigate if these viologen core distortions, induced by the helical scaffolds, lead to novel electrochemical behaviour we have studied the dication to radical cation reductions of $\mathbf{2}^{2+}$, $\mathbf{3}^{2+}$, and $\mathbf{4}^{2+}$ using cyclic voltammetry (CV) and computational studies.

2.1. Cyclic voltammetry

Representative data for each of these reductions is shown in Fig. 1. All the reductions were conducted in acetonitrile using 2 mM viologen and 0.1 M tetrabutylammonium perchlorate as the supporting electrolyte. The CVs shown in Fig. 1 were collected using a three-electrode system consisting of a glassy carbon working electrode, a platinum wire counter electrode, and a 0.1 M silver/silver nitrate reference electrode. The potentials (Fig. 1) versus the standard calomel electrode (SCE) were obtained by using ferrocene (2 mM) as an internal reference.

A pre-peak observed at a scan rate of 1000 mV/s in the CV for $\mathbf{4}^{2+}$ with glassy carbon (Fig. 1d) was missing and/or dramatically diminished in size using a platinum working electrode. (See Supplementary Information).

The current for all the other CV peaks observed during reductions of $\mathbf{2}^{2+}$, $\mathbf{3}^{2+}$, and $\mathbf{4}^{2+}$ were linearly related to the square root of the scan rate indicative of diffusion controlled processes as the source of the current. (See Supporting Information) In addition, current ratios for all the diffusion-controlled peaks in both the [4]- and [5]heli-viologens are independent of concentration ruling out contributions of bimolecular processes including the formation and subsequent oxidations of radical cation pimers.

Table 1
Relative energies (kcal/mol) of 1 and excised methyl viologens.[a]

	Dication	Radical Cation	Neutral
1	0	0	0
2	23.4	19.7	18.4
3	17.9	13.7	11.9
4	14.7	10.8	9.9

[a] Free Energies calculated at the B3LYP/6-311 + G(2d,p) computational level.

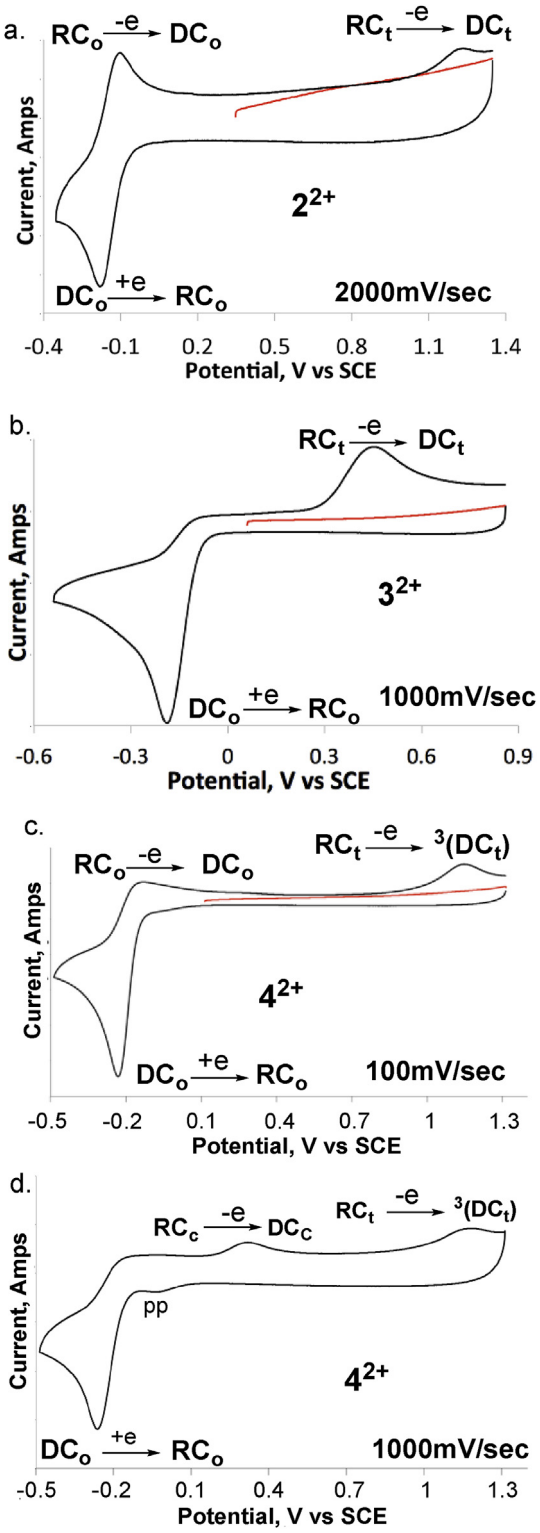

Fig. 1. Cyclic Voltammograms of 2×10^{-3} M $\mathbf{2}^{2+}$, $\mathbf{3}^{2+}$, and $\mathbf{4}^{2+}$ in acetonitrile on glassy carbon; pp: pre-peak.

These CVs (Fig. 1) demonstrate that [4]- and [5]heli-viologens $\mathbf{2}^{2+}$, $\mathbf{3}^{2+}$, and $\mathbf{4}^{2+}$ do not undergo one-electron reversible reductions by *EE* reactions typical of many viologens [5,18]. These results, however, are consistent with reductions involving transient formation of radical cation, **RC**, and dication, **DC**, skeletal isomers

initiated by intramolecular bond formation between C_1 and C_{14} in the radical cations $\mathbf{2}^{+\cdot}$ ($\mathbf{RC_o}$) and $\mathbf{3}^{+\cdot}$($\mathbf{RC_o}$) or between C_1 and C_{12} in $\mathbf{4}^{+\cdot}$($\mathbf{RC_o}$) as depicted in Fig. 2.

The structural feasibility of these bond formations leading to strained intermediates is supported by ample precedent including the formation of (2,7-dimethyl-2,7-diaza)benzo[*ghi*]-perylene bis-tetrafluoroborate, $\mathbf{5}^{2+}$ (Fig. 3), in the photochemical reaction of $\mathbf{2}^{2+}$ [21], in the formation of benzo[g,h,i]fluoranthene, **6**, during the γ -Al_2O_3 catalysed thermal reaction of 1-fluoro[4]helicene [22], and in many oxidative cyclo-dehydrogenations under Scholl reaction conditions, for example in the transformation of helicene **7** to its dehydro derivative, **8** [23]. (Fig. 3).

Fig. 2 depicts two possible stereochemically distinct mechanisms for the cyclic voltammetry results as illustrated with the reduction of $\mathbf{2}^{2+}$ in Fig. 2. These mechanisms are labelled as thermodynamic cycles **A** and **B**. Each thermodynamic/electrochemical cycle consists of a reduction, an oxidation, and two skeletal rearrangements. Both mechanisms are initiated by the one-electron reduction (shown in red) of the open viologen dication, $\mathbf{DC_o}$ ($\mathbf{2}^{2+}$($\mathbf{DC_o}$)) in Fig. 2). Thermodynamic cycle **A** involves formations of *cis*-closed radical cation, $\mathbf{RC_c}$, and *cis*-closed dication, $\mathbf{DC_c}$, intermediates, and thermodynamic cycle **B** utilizes their *trans*-closed isomers, $\mathbf{RC_t}$ and $\mathbf{DC_t}$.

The oxidation peaks appearing at +1.16 V, +0.39 V, and +1.15 V vs SCE in the CVs depicted in Fig. 1a–c, respectively, were assigned to the oxidations of the closed *trans*-radical cations, $\mathbf{RC_t}$, to form the corresponding closed dication, $\mathbf{DC_t}$ (i.e. $\mathbf{RC_t} \rightarrow \mathbf{DC_t}$). These

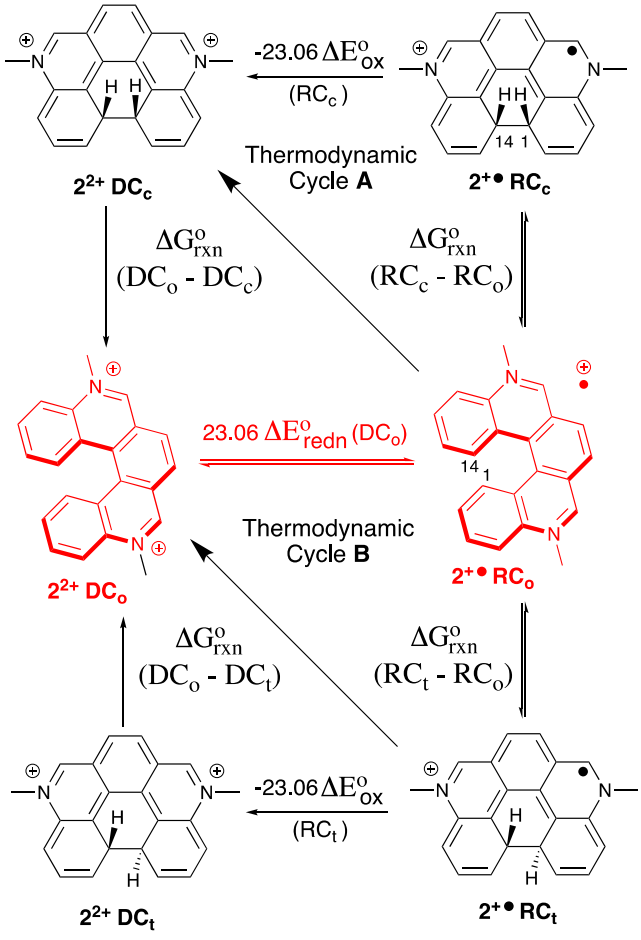

Fig. 2. Thermodynamic cycles for Reduction Mechanisms **A** and **B**. The expressions over the redox arrows represent the free energies (ΔG°) for the reactions.

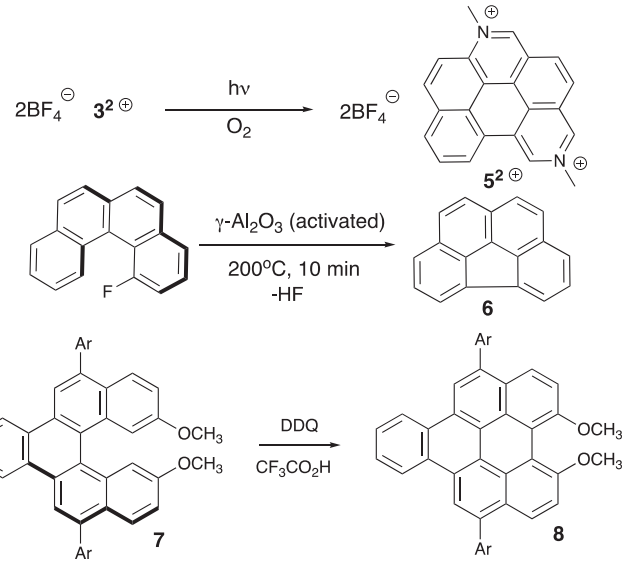

Fig. 3. Ring closures between terminal rings of helicenes.

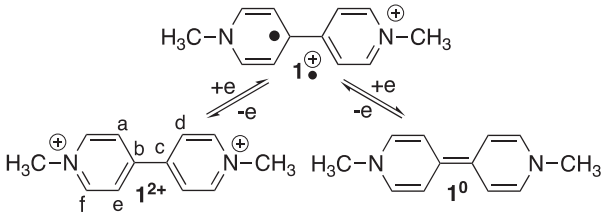

Chart 1. Methyl viologen redox states.

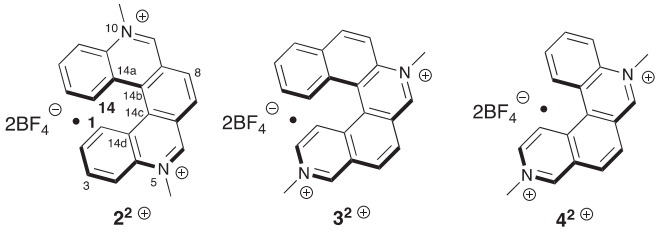

Chart 2. Structures of [4]- and [5]heli-viologens.

assignments were based on computational results (Table 2; vide infra) that show that rearrangements to the closed *trans*-radical

Table 2
Relative energies of viologens $\mathbf{2}^{2+}$, $\mathbf{3}^{2+}$, and $\mathbf{4}^{2+}$ and the other components in Mechanisms **A** and **B**.[a]

	E_{rel} (kcal/mol)		E_{rel} (kcal/mol)
	$\mathbf{2}^{2+}$	$\mathbf{3}^{2+}$	$\mathbf{4}^{2+}$
$\mathbf{DC_o}$	0	6.2	0
$\mathbf{DC_c}$	65.2	52.8	(80.5)[b](75.7)[c]
$\mathbf{DC_t}$	55.5	46.5	(73.4)[c]
$\mathbf{RC_o}$	0	0.14	0
$\mathbf{RC_c}$	51.5	42.3	63.2
$\mathbf{RC_t}$	36.6	29.8	60.4

[a] Relative Free Energies B3LYP/6-311 + G(2d,p) in acetonitrile.
[b] Singlet.
[c] Triplet.

cations, **RC$_t$** (thermodynamic cycle **B** in Fig. 2), are thermodynamically favored over rearrangements to the *cis*-radical cations, **RC$_c$**, by 14.9, 12.4, and 2.8 kcal/mol in **2**$^{2+}$, **3**$^{2+}$, and **4**$^{2+}$, respectively. This assignment receives additional support from the observation that these peaks are not observed during an initial anodic sweep (red lines in Fig. 1a–c) implying that initial generation of the helical (open) radical cation, **RC$_o$**, is required so it can act as a precursor to the **RC$_t$** intermediates. The peaks corresponding to the reductions of the viologen dication, **DC$_o$**, to the radical cation, **RC$_o$**, and the subsequent oxidation of **RC$_o$** to re-generate **DC$_o$** by the traditional *EE* mechanism are also assigned on the CV's depicted in Fig. 1a, b, 1c, and 1d. The numerical values of the reduction potentials for the quasi-reversible reductions of **2**$^{2+}$ and **4**$^{2+}$ and the peak potentials for **3**$^{2+}$ are given in column 2 of Table 3. The extended delocalization in helical viologens **2**$^{2+}$, **3**$^{2+}$, and **4**$^{2+}$ lead to decreases in their reduction potentials by the traditional *EE* mechanism ($\Delta E^{o}_{Redn}(DC_o)$ in Fig. 2) by 0.22–0.28 V in comparison to the parent bipyridinium dication, methyl viologen (−0.45 V vs SCE in CH_3CN) [24].

Viologen **4**$^{2+}$ at a scan rate of 100 mV/s (Fig. 1c) appears to have identical electrochemical behaviour to that observed for the [5] heli-viologens (compare Fig. 1a–c). However, a new peak (+0.32 V vs SCE) is observed at a scan rate of 1 V/sec (Fig. 1d) that we assign to the oxidation of the *cis*-closed radical cation, **RC$_c$**. This suggests that **4**$^{2+}$ is competitively reduced via both thermodynamic cycles **A** and **B**. Computational results that show rearrangement of **RC$_o$** to form **RC$_t$** only 2.8 kcal/mol more favorable than rearrangement to the *cis*-closed radical cation, **RC$_c$** ($_{rxn}$ = 60.4–63.2 = −2.8 kcal/mol; Table 2). provides support for this conclusion. The competitive reduction via both thermodynamic cycles **A** and **B** is also consistent with the observation of a weak but distinct peak for the **RC$_o$** → **DC$_o$** oxidation at 100 mV/s (Fig. 1c) but not at 1000 mV/s (Fig. 1d). At 100 mV/s the oxidation peak potential of the key intermediate **RC$_c$** (***RC$_c$*** ⇌ ***DC$_o$***) is not reached as rapidly as at a scan rate of 1000 mV/s allowing time for the equilibrium, (***RC$_c$*** ⇌ ***RC$_o$*** ⇌ ***RC$_t$***), between the isomeric radical cations to be established. Consequently, the concentration of **RC$_o$** is replenished in this time regime and its competitive oxidation, (**RC$_o$** → **DC$_o$**), via the typical *EE* mechanism is observed.

Finally it is useful to point out that the *cis*- (**DC$_c$**) and *trans*-closed (**DC$_t$**) dications, shown in Fig. 2 are very unstable (vide infra) and no current for their reductions are observed even when microelectrodes were used that enable very fast scan rates. These species are computationally viable (vide infra) and they most likely form during the thermodynamic cycles but they react to form the thermodynamically most stable open-dication (**DC$_o$**) at rates that prevent their direct observation. However, we cannot unambiguously rule out that direct oxidation of the *cis*- (**RC$_c$**) and *trans*-closed (**RC$_t$**) radical-cations might completely bypass the close dications to directly form the open-dication, (**DC$_o$**). (Diagonal arrows in Fig. 2).

Table 3
Redox potentials.[a]

	Helicene	$\Delta E^{o}_{redn}(DC_o)$	$\Delta E^{o}_{ox}(RC_t)$
2^{2+}	−0.18	+1.16[b](≤0.65)[c]	(≤ + 0.43)
3^{2+}	−0.25[d]	+0.39[d](≤0.28)[e]	(≤+0.02)[e]
4^{2+}	−0.18[f]	+1.19[g](≤+0.38)	+0.32[g](≤ + 0.36)

[a] Volts versus SCE in CH_3CN.
[b] Peak potential at a scan rate of 2 V/sec.
[c] Determined using Eqn. (1).
[d] Peak potential measured at a scan rate of 1 V/sec.
[e] Calculated using an estimated $\Delta E^{0}_{redn}(DC_o) = -0.18V$ vs SCE.
[f] $E_{1/2}$ measured at a scan rate of 100 mv/sec.
[g] Peak potential measured at a scan rate of 1 V/sec.

2.2. Computational studies

The open viologen dications, **DC$_o$**, and the five other reaction components, **RC$_o$**, **RC$_t$**, **DC$_t$**, **RC$_c$**, and **DC$_c$** in the two thermochemical-cycles/mechanisms have been located on the B3LYP/6-311 + G(2d,p) [25] potential energy surface in the presence of acetonitrile for all the heli-viologens shown in Chart 2 providing additional support for the reduction mechanism. (See Supporting information for computational details) The relative energies of all these reaction components are given in Table 2.

Mechanism **B** begins with the intramolecular skeletal rearrangements of the radical cations, **RC$_o$**, to form the more stable *trans*-, **RC$_t$**, rather than less stable *cis*-radical-cations. The *trans*-radical cations, however, are thermodynamically uphill by 36.6, and 29.8 kcal/mol, in **2**$^{2+}$ and, **3**$^{2+}$, respectively (Table 2). Nevertheless, in **RC$_o$** the distances between the carbon atoms (C_1 and C_{14}) that form the bond in the skeletal isomers are 3.02 Å, and 2.98 Å, in the radical cations of **2**$^{2+}$, and **3**$^{2+}$, respectively, and well within the sum of the van der Waals radii of two carbon atoms (3.40 Å) [26]. Consequently, the helicene backbone holds these two carbons at their critical collision distance enhancing the probability of population of an excited vibrational level sufficiently high in energy to traverse the activation barrier. In addition, the "clamp-like" pressure induced by the helical framework in the open radical cations of **2**$^{2+}$ and **3**$^{2+}$, are reduced by vibrations that bring the terminal rings into the bonding distance required to form the more planar closed radical cations (e.g. **RC$_t$**). The net results are extremely large effective molarities [27–30] of the terminal rings, which promote closure despite the large activation barriers [31].

Mechanism **B** is completed by the intramolecular skeletal rearrangements of the closed *trans*-dications, **DC$_t$** to regenerate **2**$^{2+}$ and **3**$^{2+}$, and are exothermic by 55.5 and 46.5 kcal/mol, respectively (Table 2). These exothermic reactions are accompanied by an increase in the C_1–C_{14} distances of 1.54 Å and 1.55 Å in **2**$^{2+}$**DC$_t$** and **3**$^{2+}$**DC$_t$** to 3.02 Å and 2.98 Å in **2**$^{2+}$**DC$_o$** and **3**$^{2+}$**DC$_o$**. Reductions of **2**$^{2+}$ and **3**$^{2+}$ by mechanism **B** are completely reversible and repetitive cyclic voltammetry (CV) cycles of these reactions occur without any significant decrease in current at any potential.

The reduction of the [4]heli-viologen, **4**$^{2+}$, however, is very different than that of **2**$^{2+}$ and **3**$^{2+}$ for several reasons. First, the additional strain (i.e. total strain not viologen core distortional strain vide supra) in the closed radical cation and dication intermediates, leads to a significant increase in the endothermicity of the radical cation ring closure and to the exothermicity of the closed dication ring opening (Table 2). In addition, the C_1–C_{12} bond length in the minimum energy closed *cis*-dication (1.61 Å), *trans*-dication (1.60 Å), *cis*-radical-cation (1.61 Å), and *trans*-radical-cation (1.60 Å), are 0.06 ± 0.04 Å longer than in their homologues in the reactions of **2**$^{2+}$ and **3**$^{2+}$. The strain in the *cis*-radical cation and *cis*-dication closed intermediates also lead to adoption of a corannulene-like bowl structure devoid of one of the rim aromatic rings (Chart 3).

The *cis*- and *trans*-closed dication, **DC$_c$** and **DC$_t$**, isomers of [4] heli-viologen, **4**$^{2+}$**(DC$_o$)** (Chart 3), cannot be written as classical Kekulé structures. Consequently, they can potentially exist as either singlet or triplet ground states. Indeed, the triplet, *cis*-closed dication [3],**(DC$_c$)**, is 4.8 kcal/mol more stable than the singlet *cis*-dication [1],**(DC$_c$)**. However, all attempts to locate the singlet *trans*-closed dication [1],**(DC$_t$)**, for comparison to its triplet in CH_3CN or in the gas phase resulted in ring cleavage and optimization to form the open **4**$^{2+}$(**DC$_o$**) dication (Fig. 2).

The initial skeletal rearrangements of **RC$_O$** in the reductions of **4**$^{2+}$ via mechanisms **B** and **C** are 24–31 kcal/mol more endothermic than the analogous closures encountered during reductions of **2**$^{2+}$ and **3**$^{2+}$. However, the distance between C_1 and C_{12} in **RC$_o$** (3.08 Å)

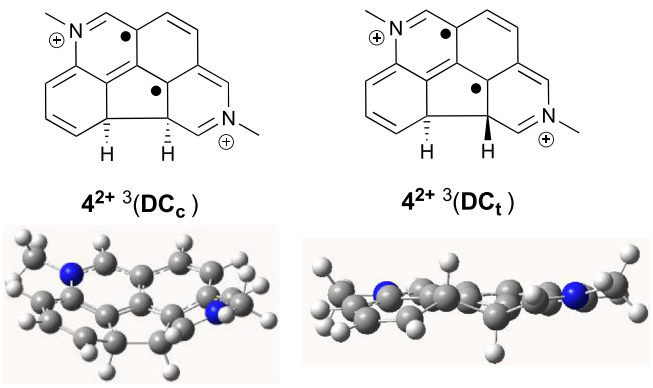

Chart 3. Triplet ground state *cis*- and *trans*-closed $\mathbf{3}^{2+}$ $^3(\mathbf{DC_c})$ and $\mathbf{3}^{2+}$ $^3(\mathbf{DC_t})$.

is also well within the sum of the van der Waals radii of two carbon atoms (3.40 Å) and the decrease in the distance upon closure (1.48 Å) is identical in the reductions of $\mathbf{2}^{2+}$ and $\mathbf{4}^{2+}$ and only slightly longer than in the reduction of $\mathbf{3}^{2+}$ (1.43 Å).

Not surprisingly the oxidations of the *trans*-closed radical cations are irreversible in all of the reactions and the oxidation of the *cis*-closed radical cation is irreversible in the reduction of $\mathbf{4}^{2+}$ since the opening of the closed dication products, $\mathbf{DC_t}$ and $\mathbf{DC_c}$ to form the viologens are so exothermic. Nevertheless, three-legs of thermodynamic cycle **B** are known for $\mathbf{2}^{2+}$. Consequently, Eqn. (1), in which C_x is C_t describes the energy change in thermodynamic cycle **B** in Fig. 2 and was used to calculate the maximum possible value of the thermodynamically significant standard oxidation potential, $\Delta E^o_{ox}(RC_t)$ as shown in Table 2 in parentheses. If $\Delta E^o_{ox}(RC_t)$ were greater than this value the ECEC reaction depicted in Fig. 1 would not be thermodynamically feasible (Eqn. (1)) and would not be observed.

$$\Delta E^o_{ox}(RC_x) = -[\Delta G^o(DC_o - DC_x) + \Delta G^o(RC_x - RC_o)]/23.06 + \Delta E^o_{redn}(DC_o) \quad (1)$$

The calculated maximum value of the standard oxidation potential for $\mathbf{RC_t}$ formed in the reduction of $\mathbf{3}^{2+}$ is 370 mV smaller than in the reaction of $\mathbf{2}^{2+}$ (Table 3). This is qualitatively consistent with the observation that the oxidation peak potential in $\mathbf{3}^{2+}$ is 770 mV smaller than in $\mathbf{2}^{2+}$ (Fig. 1).

3. Summary

All of the heli-viologens (Table 3) are reduced easier than methyl viologen ($E_{1/2} = -0.44$ V vs SCE) [5] consistent with the greater delocalization of the charge and spin density in the π-extended helical viologen radical cations. Methyl viologen is also reduced by a simple 1-electron (*EE*) mechanism and the [5]heli-viologens react via a high effective molarity driven square (ECEC)-mechanism [32] depicted by thermodynamic cycle **B**. In contrast, the very small difference in thermodynamic stability of the *cis*- and *trans*-closed radical cations ($\mathbf{RC_c}$ and $\mathbf{RC_t}$) formed in the reduction of the [4]heli-viologen, $\mathbf{4}^{2+}$, allow competitive ECEC reductions via both thermodynamic cycles **A** and **B** to be observed (Fig. 2). The *trans*-closed and *cis*-closed dications, $\mathbf{DC_t}$ and $\mathbf{DC_c}$, were not experimentally detected because of their very large exothermic conversions to their viologen $\mathbf{2}^{2+}$, $\mathbf{3}^{2+}$, or $\mathbf{4}^{2+}$, precursor. Nevertheless, both the triplet closed dication formed during reduction of $\mathbf{4}^{2+}$, and the singlet closed dications formed in the reductions of $\mathbf{2}^{2+}$ and $\mathbf{3}^{2+}$ are minima on the B3LYP/6−311+(2d,p) potential energy surface.

Finally, the robust chemical and electrochemical behaviors of these chiral viologens portend well for their future incorporation into viologen based new materials. In particular, they could function as potentially chiral replacements for methyl viologen in blue box (Chart 4A). Alternatively, as a result of significant contraction-extension of up to 1.5–2.0 Å measured parallel to the helical axis during formation-cleavage cycles of the C_1–C_{14} bonds, they are attractive candidates for components of molecular muscles [33] (Chart 4B).

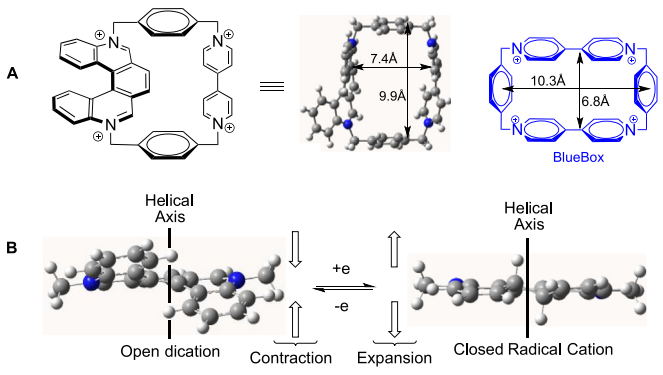

Chart 4. A. A chiral blue box. **B.** A molecular muscle.

Competing financial interests

The authors declare no competing financial interest.

Acknowledgements

We thank the United States National Science Foundation (CHE-1147542 and CHE-1762161) for their generous support of this research.

Appendix A. Supplementary data

Supplementary data to this article can be found online at https://doi.org/10.1016/j.tet.2019.04.043.

References

[1] H. Weidel, M. Russo, Monatshefte 3 (1882) 850–885.
[2] C. Kurniawan, H. Noguchi, T. Masuda, K. Uosaki, Electrochem. Commun. 62 (2016) 56–59.
[3] H. Noh, C.-W. Kung, K.-i. Otake, A.W. Peters, Z. Li, Y. Liao, X. Gong, O.K. Farha, J.T. Hupp, ACS Catal. 8 (2018) 9848–9858.
[4] L.A. Summers, The Bipyridinium Herbicides, Academic Press, New York, N. Y., 1980.
[5] P.M.S. Monk, The Viologens. Physicochemical Properties, Synthesis and Applications of the Salts of 4, 4'-Bipyridine, John Wiley & Sons, Chichester, England, 1998.
[6] A.R. Bernardo, J.F. Stoddart, A.E. Kaifer, J. Am. Chem. Soc. 114 (1992) 10624–10631.
[7] C.J. Bruns, M. Frasconi, J. Iehl, K.J. Hartlieb, S.T. Schneebeli, C. Cheng, S.I. Stupp, J.F. Stoddart, J. Am. Chem. Soc. 136 (2014) 4714–4723.
[8] E.J. Dale, D.P. Ferris, N.A. Vermeulen, J.J. Henkelis, I. Popovs, M. Juríček, J.C. Barnes, S.T. Schneebeli, J.F. Stoddart, J. Am. Chem. Soc. 138 (2016) 3667–3670.
[9] E.J. Dale, N.A. Vermeulen, A.A. Thomas, J.C. Barnes, M. Jur√≠çek, A.K. Blackburn, N.L. Strutt, A.A. Sarjeant, C.L. Stern, S.E. Denmark, J.F. Stoddart, J. Am. Chem. Soc. 136 (2014) 10669–10682.
[10] E.L. Clennan, Coord. Chem. Rev. 248 (2004) 477–492.
[11] A.M. Brun, A. Harriman, J. Am. Chem. Soc. 113 (1991) 8153–8159.
[12] M. Asakawa, W. Dehaen, G. L'abbé, S. Menzer, J. Nouwen, F.M. Raymo, J.F. Stoddart, D.J. Williams, J. Org. Chem. 61 (1996) 9591–9595.
[13] B. Odell, M.V. Reddington, A.M.Z. Slawin, N. Spencer, J.F. Stoddart, D.J. Williams, Angew Chem. Int. Ed. Engl. 27 (1988) 1547–1550.
[14] C.-H. Sue, S. Basu, A.C. Fahrenbach, A.K. Shveyd, S.K. Dey, Y.Y. Botros, J.F. Stoddart, Chem. Sci. 1 (2010) 119–125.
[15] J.C. Barnes, M. Jurícek, N.L. Strutt, M. Frasconi, S. Sampath, M.A. Giesener, P.L. McGrier, C.J. Bruns, C.L. Stern, A.A. Sarjeant, J.F. Stoddart, J. Am. Chem. Soc.

135 (2013) 183–192.
[16] S. Cantekin, A.J. Markvoort, J.A.A.W. Elemans, A.E. Rowan, R.J.M. Nolte, J. Am. Chem. Soc. 137 (2015) 3915–3923.
[17] H.S. Farwaha, G. Bucher, J.A. Murphy, Org. Biomol. Chem. 11 (2013) 8073–8081.
[18] C.L. Bird, A.T. Kuhn, Chem. Soc. Rev. 10 (1981) 49–83.
[19] S. Hünig, J. Groβ, E.F. Lier, H. Quast, Justus Liebigs Ann. Chem. 1973 (1973) 339–358.
[20] M.R. Geraskina, A.S. Dutton, M.J. Juetten, S.A. Wood, A.H. Winter, Angew. Chem. Int. Ed. 56 (2017) 9435–9439.
[21] X. Zhang, E.L. Clennan, N. Arulsamy, R. Weber, J. Weber, J. Org. Chem. 81 (2016) 5474–5486.
[22] K.Y. Amsharov, P. Merz, J. Org. Chem. 77 (2012) 5445–5448.
[23] J.-D. Chen, H.-Y. Lu, C.-F. Chen, Chem. Eur J. 16 (2010) 11843–11846.
[24] U. Ammon, C. Chiorboli, W. Dümler, G. Grampp, F. Scandola, H. Kisch, J. Phys. Chem. A 101 (1997) 6876–6882.
[25] R.A. Gaussian 09, M.J. Frisch, G.W. Trucks, H.B. Schlegel, G.E. Scuseria, M.A. Robb, J.R. Cheeseman, G. Scalmani, V. Barone, B. Mennucci, G.A. Petersson, H. Nakatsuji, M. Caricato, X. Li, H.P. Hratchian, A.F. Izmaylov, J. Bloino, G. Zheng, J.L. Sonnenberg, M. Hada, M. Ehara, K. Toyota, R. Fukuda, J. Hasegawa, M. Ishida, T. Nakajima, Y. Honda, O. Kitao, H. Nakai, T. Vreven, J.A. Montgomery Jr., J.E. Peralta, F. Ogliaro, M. Bearpark, J.J. Heyd, E. Brothers, K.N. Kudin, V.N. Staroverov, R. Kobayashi, J. Normand, K. Raghavachari, A. Rendell, J.C. Burant, S.S. Iyengar, J. Tomasi, M. Cossi, N. Rega, J.M. Millam, M. Klene, J.E. Knox, J.B. Cross, V. Bakken, C. Adamo, J. Jaramillo, R. Gomperts, R.E. Stratmann, O. Yazyev, A.J. Austin, R. Cammi, C. Pomelli, J.W. Ochterski, R.L. Martin, K. Morokuma, V.G. Zakrzewski, G.A. Voth, P. Salvador, J.J. Dannenberg, S. Dapprich, A.D. Daniels, O. Farkas, J.B. Foresman, J.V. Ortiz, J. Cioslowski, D.J. Fox, Gaussian, Inc., Wallingford CT, 2009.
[26] A. Bondi, J. Phys. Chem. 68 (1964) 441–451.
[27] S. Di Stefano, R. Cacciapaglia, L. Mandolini, Eur. J. Org. Chem. 2014 (2014) 7304–7315.
[28] C. Galli, L. Mandolini, Eur. J. Org. Chem. 2000 (2000) 3117–3125.
[29] R. Karaman, Bioorg. Chem. 38 (2010) 165–172.
[30] F.M. Menger, A.L. Galloway, D.G. Musaev, Chem. Commun. (2003) 2370–2371, https://doi.org/10.1039/B306342A.
[31] We cannot rule out the possibility that heavy atom tunnelling might also contribute the rate of intra-molecular closure of the radical cation intermediates. a C. Doubleday, R. Armas, D. Walker, C.V. Cosgriff, E.M. Greer, Angew. Chem. Int. Ed. 56 (2017) 13099–13102;
b C.S. Michel, P.P. Lampkin, J.Z. Shezaf, J.F. Moll, C. Castro, W.L. Karney, Tunneling by 16 carbons: planar bond shifting in [16]Annulene, J. Am. Chem. Soc. 141 (2019) 5286–5293, https://doi.org/10.1021/jacs.8b13131.
[32] A. Khan, X. Lu, L. Aldous, C. Zhao, J. Phys. Chem. C 117 (2013) 18334–18342.
[33] C.J. Bruns, J.F. Stoddart, Acc. Chem. Res. 47 (2014) 2186–2199.